

Husimi–Wigner representation of chaotic eigenstates

BY FABRICIO TOSCANO^{1,2}, ANATOLE KENFACK³, ANDRE R. R. CARVALHO⁴,
JAN M. ROST³ AND ALFREDO M. OZORIO DE ALMEIDA^{5,*}

¹*Fundação Centro de Ciências e Educação Superior a Distância do Estado do Rio de Janeiro, 20943-001 Rio de Janeiro, RJ, Brazil*

²*Instituto de Física, Universidade Federal do Rio de Janeiro, Caixa Postal 68528, 21941-972 Rio de Janeiro, RJ, Brazil*

³*Max-Planck-Institut für Physik Komplexer Systeme, Nöthnitzer Strasse 38, 01187 Dresden, Germany*

⁴*Department of Physics, Faculty of Science, The Australian National University, Canberra, ACT 0200, Australia*

⁵*Centro Brasileiro de Pesquisas Físicas, Rua Xavier Sigaud 150, 22290-180 Rio de Janeiro, RJ, Brazil*

Just as a coherent state may be considered as a quantum point, its restriction to a factor space of the full Hilbert space can be interpreted as a quantum plane. The overlap of such a factor coherent state with a full pure state is akin to a quantum section. It defines a reduced pure state in the cofactor Hilbert space. Physically, this factorization corresponds to the description of interacting components of a quantum system with many degrees of freedom and the sections could be generated by conceivable partial measurements.

The collection of all the Wigner functions corresponding to a full set of parallel quantum sections defines the Husimi–Wigner representation. It occupies an intermediate ground between the drastic suppression of non-classical features, characteristic of Husimi functions, and the daunting complexity of higher dimensional Wigner functions. After analysing these features for simpler states, we exploit this new representation as a probe of numerically computed eigenstates of a chaotic Hamiltonian. Though less regular, the individual two-dimensional Wigner functions resemble those of semiclassically quantized states.

Keywords: phase space representations; Wigner function; Husimi function; semiclassical mechanics; chaotic eigenstates

1. Introduction

It is well known that phase space representations of quantum mechanics are powerful tools for studying the correspondence between the density operator and classical distributions in phase space. The several choices of representation are partially distinguished by the different ways they highlight classical

* Author for correspondence (ozorio@cbpf.br).

structures against a background of quantum interferences. In the case of the Wigner function (Wigner 1932), $W(\mathbf{x})$, in terms of the phase space variables, $\mathbf{x} = (\mathbf{x}_1, \dots, \mathbf{x}_L) = (p_1, \dots, p_L, q_1, \dots, q_L)$, the oscillations due to interferences may even have higher amplitudes than the classical region. By contrast, the Husimi function (Husimi 1940; Takahashi 1986), which may be defined as a coarse graining of the Wigner function,¹

$$\mathcal{H}(\mathbf{X}) = (\pi\hbar)^{-L} \int d\mathbf{x} W(\mathbf{x}) \exp\frac{-(\mathbf{x} - \mathbf{X})^2}{\hbar}, \quad (1.1)$$

subtly disguises information on quantum coherences to the point that they may be numerically undetectable, while clearly displaying most classical structures (Toscano & Ozorio de Almeida 1999).

In the case of $(2L)$ -dimensional phase spaces, with $L > 1$, the approximate classical support for a quantum state may take the form of a discrete set of points. These correspond to either a coherent state, squeezed or not, or their superposition, sometimes known as *Schrödinger cat states*. Alternatively, semiclassical *Van Vleck states* (Van Vleck 1928) correspond to L -dimensional (Lagrangian) surfaces. Of even higher dimension is the support of *ergodic states* satisfying Schnirelman's theorem (Schnirelman 1974; Colin de Verdière 1985; Zelditch 1987): eigenstates of (classically) chaotic Hamiltonians, supported by the full $(2L-1)$ -dimensional energy shell. Of course, all these types of state can be superposed in various ways, which, in their turn, produce new interferences.

Even though we cannot directly visualize such classical structures in a higher dimensional phase space, they will show up in appropriate two-dimensional sections of the corresponding Husimi function. Indeed, we may follow Kurchan et al. (1989) and identify classical phase space structures relating to a quantum state as those onto which the Husimi function condenses. Even so, it will be virtually impossible to extricate the crucial quantum phase information in this representation, unless all analytical properties concerning the state are known (Leboeuf & Voros 1990, 1995). The situation for the Wigner function is just the opposite: all phase information is immediately available in the oscillatory interference pattern, but it becomes hard to sort out its embarrassing richness. For example, a two-dimensional section may contain a (plain) periodic orbit. States that are *scarred* by this periodic orbit (Heller 1984; Bogomolny 1988; Berry 1989) are clearly distinguishable in the section of the Wigner function through this plane (Toscano et al. 2001). Nonetheless, interferences also arise which can only be generated by classical structures that are nowhere near this two-dimensional plane. There is certainly a need for a more manageable representation of the interference effects that decorate classical structures of general pure states. Indeed, the Wigner function itself, in the simple case that $L=1$, is a good example of a comprehensible interference pattern (Berry 1977a).

Needless to say, other representations have their merits, depending on the intended application. However, the position representation represents only a scar of the projection of a given periodic orbit onto the position plane, where it must be unravelled from multiple intersections with other orbit projections, as well as

¹Here and throughout, we make the convenient choice that the frequency of the harmonic oscillator for the coherent states is $\omega = m=1$.

being coloured by self-interference and focalization. Other useful representations, such as the harmonic oscillator basis, are certainly much more opaque, as far as distinguishing classical phase space features from quantum interferences.

Our purpose here is to develop a new tool for the analysis of the chaotic eigenstates of higher dimensional systems. Even though there has been continuing interest in their localization and statistical properties, starting with Voros (1976) and Berry (1977*b*), subsequent work in this field has concentrated on the description of chaotic eigenstates of quantum maps (Leboeuf & Voros 1990, 1995; Hannay 1998; for many further references in this field, see Schanz (2005)). The reason for this is precisely to avoid the difficulties of coping with higher dimensions. The detailed analysis of ergodic states for $L > 1$ is still in its preliminary stages. Their Husimi functions should be concentrated in a narrow neighbourhood of the energy shell, but the often repeated statement that this also holds for the Wigner function is false. Indeed, it has been shown by Ozorio de Almeida *et al.* (2004) that all large-scale pure states must have correspondingly small-scale oscillations in their Wigner functions. Such *sub-Planckian structures* (Zurek 2001) do not contribute to the averages of smooth observables (hence, the ergodicity over the energy shell). However, future refinements of experimental techniques will inevitably lead to measurable interference effects. Here, we introduce a conceptual tool with which to probe into the details of these higher dimensional states.

The joint Husimi–Wigner representation of quantum mechanics, *huwi representation* for short, avoids the extremes of near-classicality, or of excessive quantum complexity, that characterize alternatively its parent representations. Decomposing the phase space variables in the Wigner function, $W(\mathbf{x})$, as $\mathbf{x} = (\mathbf{x}_1, \mathbf{x}')$, with $\mathbf{x}' = (\mathbf{x}_2, \dots, \mathbf{x}_L)$, and specifying a two-dimensional plane by the $2(L-1)$ equations, $\mathbf{x}' = \mathbf{X}' = \text{const.}$, the huwi function is defined as

$$hw_{\mathbf{X}'}(\mathbf{x}_1) = (\pi\hbar)^{-(L-1)} \int d\mathbf{x}' W(\mathbf{x}_1, \mathbf{x}') \exp \frac{-(\mathbf{x}' - \mathbf{X}')^2}{\hbar}. \quad (1.2)$$

In §2, the general features of this complete representation of the density operator in the phase space, $(\mathbf{x}_1, \mathbf{X}')$, are discussed. However, our main focus will be centred on the huwi function for a given choice of \mathbf{X}' . Viewed classically, this would be merely a slight thickening of a plane section of the Wigner function, but it is a truly quantum section; that is, for each parameter, \mathbf{X}' , $hw_{\mathbf{X}'}(\mathbf{x}_1)$ represents a different pure state. All of these states belong to the same factor Hilbert space, which corresponds to the phase plane, \mathbf{x}_1 . Besides this geometric point of view, quantum sections can also be interpreted as resulting from conceivable experiments, effected on all degrees of freedom, except the one corresponding to the phase plane, \mathbf{x}_1 . The average of all such experimental probes defines the partial trace, which is central to the study of bipartite entanglement (e.g. Mintert *et al.* 2005).

In §3, we discuss the huwi representation in the simple case of coherent states and their superposition. This already exemplifies the convenient way in which the thickened section erases, not only the classical regions foreign to the section, but also all their interference effects. This is also the clearest setting in which to discuss rotations and other classical canonical transformations as tools to bring desired features into view. Van Vleck states are then analysed in §4. It is shown

that, generically, their huwi representation can be approximated by Gaussians in the \mathbf{x}_1 phase plane, corresponding to (squeezed) coherent states, or generalized Schrödinger cat states, centred on the discrete set of points where the constant \mathbf{X}' -plane intersects the classical surface.

The final aim is to understand the phase space structure of higher dimensional eigenstates of quantized chaotic systems, which is still an open problem in physics and mathematics. Ergodic states have so far evaded any compact analytical characterization in any representation, but eigenstates of general Hamiltonians with predominantly chaotic classical motion may be even harder to describe. As a first example, we present a computational study in §5 of the eigenstates of such a (quartic) Hamiltonian in a four-dimensional phase space. Given that the two-dimensional section of a compact $(2L - 1)$ -dimensional energy shell is a closed curve, we investigate the family resemblance between $hw_{\mathbf{X}'}(\mathbf{x}_1)$ and the eigenstates of a Hamiltonian in a two-dimensional phase space, defined so that its level curve coincides with the section of the higher dimensional energy shell. The computational huwi patterns discussed in §6 suggest that, though these new kinds of pure states somewhat resemble familiar semiclassical states that satisfy Bohr–Sommerfeld quantization, they exhibit amplitude fluctuations and phase dislocations in their two-dimensional Wigner functions that resemble those found in the wave trains of short pulses (Nye & Berry 1974).

2. Quantum sections

Coherent states, $|\mathbf{X}\rangle$, defined in the position representation as

$$\langle q|\mathbf{X}\rangle = \left(\frac{1}{\pi\hbar}\right)^{L/4} \exp\left(-\frac{1}{2\hbar}(q-Q)^2 + \frac{i}{\hbar}P\cdot\left(q - \frac{Q}{2}\right)\right), \quad (2.1)$$

form a basis for the Hilbert space that is overcomplete (Glauber 1963; Sudarshan 1963; Cohen Tannoudji et al. 1977; Klauder & Skagerstam 1985; Perelomov 1986; Schleich 2001). The Husimi function can be defined directly in terms of coherent states, alternatively to (1.1). Given the density operator for a pure state as $\hat{\rho} = |\psi\rangle\langle\psi|$, then

$$\mathcal{H}_\psi(\mathbf{X}) = \langle\mathbf{X}|\hat{\rho}|\mathbf{X}\rangle = \text{tr } \hat{\rho}|\mathbf{X}\rangle\langle\mathbf{X}| = |\langle\mathbf{X}|\psi\rangle|^2. \quad (2.2)$$

Considering the full Hilbert space as a tensor product of factor spaces, $\mathbf{H} = \mathbf{H}_1 \otimes \dots \mathbf{H}_l \otimes \dots \mathbf{H}_L$, for each of the L degrees of freedom, the coherent state basis also factors, i.e.

$$|\mathbf{X}\rangle = |\mathbf{X}_1\rangle \otimes \dots |\mathbf{X}_l\rangle \otimes \dots |\mathbf{X}_L\rangle. \quad (2.3)$$

Therefore, decomposing again $\mathbf{X} = (\mathbf{X}_1, \mathbf{X}')$ and taking the partial overlaps,

$$|\mathbf{X}_1\rangle = \langle\mathbf{X}'|\mathbf{X}\rangle = |\mathbf{X}_1\rangle\langle\mathbf{X}_2|\mathbf{X}_2\rangle \dots \langle\mathbf{X}_L|\mathbf{X}_L\rangle \quad (2.4)$$

generates a basis for the factor space, \mathbf{H}_1 , such that each $|\psi_{\mathbf{X}'}\rangle = \langle\mathbf{X}'|\psi\rangle$ is a pure state with its wave function,

$$\langle\mathbf{X}'|\psi\rangle(q_1) = \int dq' \langle q'|\mathbf{X}'\rangle^* \langle q_1, q'|\psi\rangle. \quad (2.5)$$

The partial overlap of both the bra and the ket of $\hat{\rho} = |\psi\rangle\langle\psi|$ with the same factor coherent state, $|\mathbf{X}'\rangle$, defines a reduced density operator,

$$\hat{\rho}_{\mathbf{X}'} = \langle\mathbf{X}'|\rho|\mathbf{X}'\rangle, \tag{2.6}$$

in the factor Hilbert space \mathbf{H}_1 . This is henceforth referred to as a *quantum section*.

If this state is represented by its Husimi function, then

$$\mathcal{H}_{\mathbf{X}'}(\mathbf{x}_1) = \mathcal{H}(\mathbf{x}_1, \mathbf{X}'), \tag{2.7}$$

i.e. the Husimi function for this quantum section is just the section of the full Husimi function. This should not be confused with the *quantum Poincaré surface of section* (Leboeuf & Saraceno 1990a,b), which is discussed in §5. Recalling now that the Wigner function in the full phase space is defined as (Royer 1977; Ozorio de Almeida 1998)

$$W(\mathbf{x}) = (\pi\hbar)^{-L} \text{tr} \hat{\rho} \hat{R}_{\mathbf{x}}, \tag{2.8}$$

where the operator for the reflection through the point \mathbf{x} is

$$\hat{R}_{\mathbf{x}} = 2^{-L} \int dQ \left| q - \frac{Q}{2} \right\rangle \left\langle q - \frac{Q}{2} \right| e^{ip \cdot Q/\hbar} \tag{2.9}$$

and that similar definitions hold for Wigner functions defined in subspaces, with the appropriate adaptation of notation. Then, we find that the alternative definition for the huwi function,

$$hw_{\mathbf{X}'}(\mathbf{x}_1) = (\pi\hbar)^{-1} \text{tr} \hat{\rho}_{\mathbf{X}'} \hat{R}_{\mathbf{x}_1} = (\pi\hbar)^{-1} \text{tr} \hat{\rho} [\hat{R}_{\mathbf{x}_1} \otimes |\mathbf{X}'\rangle\langle\mathbf{X}'|], \tag{2.10}$$

is equivalent to (1.2).

Clearly, the case of product states,

$$|\psi\rangle = |\psi_1\rangle \otimes |\psi'\rangle, \tag{2.11}$$

leads to products of the representations of the factor states. Thus, the huwi representation is only of interest for states in which the component described in the factor Hilbert space, \mathbf{H}_1 , is entangled with the \mathbf{H}' component.

In the case of interacting particles, or entangled modes of the electromagnetic field (beams) in the optical analogy, the huwi function associated with the factor state in \mathbf{H}_1 , for a particle with a single degree of freedom (or a single optical mode), can be measured by a conceivable experiment. For simplicity, let us consider two entangled particles or entangled optical modes.² In the optical context, the celebrated thought experiment of Arthurs & Kelly (1965) for the approximate simultaneous measurement of the field quadratures p' and q' of one of the modes (corresponding to the momentum p' and position q' of a particle) can be realized experimentally. Leonhardt (1997) reviews the relevant literature and shows that these experiments effectively measure the Husimi function. The same reference also discusses quantum tomography as an experimental method for the measurement of Wigner functions. Applying this method to the measurement of other entangled mode (or particle), corresponding to the phase space, $\mathbf{x}_1 = (p_1, q_1)$, the huwi function can, in principle, be experimentally reconstructed with the existing technology in quantum optics.

In this light, the sections that generate lower dimensional phase space representations acquire a physical, as well as a geometric, interpretation. The pure states resulting from each section coincide with those revealed by a

²The two entangled photon beams could be the result of a parametric down conversion (see Howell *et al.* 2004).

conceivable experimental probe acting on the complementary coupled system. The average of all such measurements can be identified with the *partial trace*: $\hat{\rho}_1 = \text{tr}'\hat{\rho}$. This is also a density operator, albeit not pure. The corresponding Wigner function is known to be

$$W_1(\mathbf{x}_1) = (\pi\hbar)^{-1} \text{tr} \rho[\hat{R}_{\mathbf{x}_1} \otimes \hat{I}'] = \int d\mathbf{x}' W(\mathbf{x}_1, \mathbf{x}'), \quad (2.12)$$

where \hat{I} is the identity operator.

The definition of the huwi function is based on a wide, but rarely used, freedom in the choice of representations of tensor products of Hilbert spaces. These correspond classically to Cartesian products of phase planes and it is more usual to exploit alternative generating functions for canonical transformations by exchanging variables in classical mechanics (Arnold 1978; Goldstein 1980). However, the corresponding matrix elements in quantum mechanics,

$$\langle q_1, p_2, \dots | \hat{A} | p'_1, p'_2, \dots \rangle = \text{tr} \hat{A} [|p'_1\rangle \langle q_1| \otimes |p'_2\rangle \langle p_2| \otimes \dots], \quad (2.13)$$

also form a faithful representation of the operator \hat{A} , for all choices of either p_j or q_j , and of p'_j or q'_j . Furthermore, it is possible to include operators $\hat{R}_{\mathbf{x}_j}$ in the same class as the dyadic operators $|p'_j\rangle \langle q_j|$ as a faithful basis for representing operators. Indeed, they may be interpreted as merely defining alternative planes in the doubled phase space that corresponds to operators, just as the ordinary phase space corresponds to the Hilbert space (e.g. Ozorio de Almeida 2006). Alternatively, the Husimi basis, $|\mathbf{X}_j\rangle \langle \mathbf{X}_j|$, can also be used for any of the degrees of freedom. In the context of classical generating functions, switches of representation are usually motivated by the need to avoid singularities, i.e. caustics, in the implicit definition of the transformation. These are also a problem for semiclassical approximations to quantum evolution. In the present context, the huwi representation is singled out by the clarity with which it exhibits both classical and quantum characteristics of a pure state.

A point of practical importance concerns normalization. Definition (2.6) should be divided by $N(\mathbf{X}') = \text{tr}_1 \hat{\rho}_{\mathbf{X}'}$, so as to represent a normalized density operator. Thus, the integral of $hw_{\mathbf{X}'}(\mathbf{x}_1)$ over all \mathbf{x}_1 is $N(\mathbf{X}')$. We have left this normalization factor out of the definition, because the basic interest is in the description of the full state in the higher dimensional phase space. Indeed, for bound states, there will be whole ranges of the parameters \mathbf{X}' for which the overlap of the partial coherent state with $|\psi\rangle$ will be negligible, so that $N(\mathbf{X}')$ becomes a small divisor. It will be verified in the following sections that this occurs where the classical plane, $\mathbf{x}' = \mathbf{X}'$, is not even close to intersecting the classical support of $|\psi\rangle$.

So far, we have not considered the possibility of squeezing the coherent states $|\mathbf{X}'\rangle$, which generate the huwi function. In the limit of infinite squeezing, these will be replaced by the position states $|Q'\rangle$, so that equation (2.5) for the wave function in the factor space becomes simply

$$\langle Q' | \psi \rangle (q_1) = \int dq' \langle q' | Q' \rangle^* \langle q_1, q' | \psi \rangle = \langle q_1, Q' | \psi \rangle. \quad (2.14)$$

The corresponding Wigner function is just the limiting form of the huwi function

$$hw_{Q'}(\mathbf{x}_1) = \int d\mathbf{x}' W(\mathbf{x}_1, \mathbf{x}') \delta(q' - Q'). \quad (2.15)$$

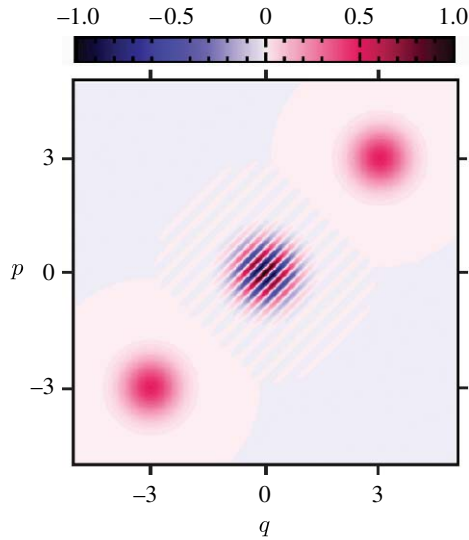


Figure 1. The Wigner function for the Schrödinger cat state displays a pair of classical Gaussians, one for each coherent state, and a third Gaussian modulated by interference fringes halfway between the pair. If we identify $q=q_1$ and $p=p_1$, this will be also the huwi function of the multidimensional Schrödinger cat state (1.2) corresponding to the quantum section $\mathbf{X}'_a = \mathbf{X}'_b = \mathbf{X}'$.

Hence, this limit results from a combined momentum projection of the p' , with a (thin) section of the positions, q' . In the case of a four-dimensional phase space, only one variable $q' = Q'$ is fixed, so this has become a three-dimensional section.

3. Superposition of coherent states

It is well known that the coherent states (2.1) have Gaussian Wigner functions (e.g. Ozorio de Almeida 1998; Schleich 2001), whereas a superposition of coherent states, $|\mathbf{X}_a\rangle \pm |\mathbf{X}_b\rangle$, sometimes known as a Schrödinger cat state, has the Wigner function

$$\begin{aligned}
 W_{\pm}(\mathbf{x}) &= \frac{1}{[2\pi\hbar(1 \pm \exp(-(\mathbf{X}_a - \mathbf{X}_b)^2/\hbar))]^L} \\
 &\times \left[\exp(-(\mathbf{x} - \mathbf{X}_a)^2/\hbar) + \exp(-(\mathbf{x} - \mathbf{X}_b)^2/\hbar) \right. \\
 &\left. \pm 2 \exp(-(\mathbf{x} - (\mathbf{X}_a + \mathbf{X}_b)/2)^2/\hbar) \cos \frac{1}{\hbar} \mathbf{x} \wedge (\mathbf{X}_a - \mathbf{X}_b) \right]. \quad (3.1)
 \end{aligned}$$

It consists of two classical Gaussians centred on \mathbf{X}_a and \mathbf{X}_b , together with an interference pattern with a Gaussian envelope centred on their midpoint, as shown in figure 1. The spatial frequency of this oscillation increases with the separation $|(\mathbf{X}_a - \mathbf{X}_b)|$. Increasing the number of coherent states merely increases the number of classical Gaussians and adds new localized interference patterns midway between each pair.

The overall picture does not depend on L , the number of degrees of freedom. Suppose then that L is large and that we study classical two-dimensional sections, $\mathbf{x}' = \mathbf{X}'$, of the Wigner function of a superposition of a pair of coherent states that

are centred on arbitrary points \mathbf{X}_j . Clearly, $W(\mathbf{x}_1, \mathbf{X}')$ will only be appreciable if the chosen \mathbf{X}' -plane is close to one of the \mathbf{X}'_j -planes on which the coherent states lie, or close to $(\mathbf{X}'_j + \mathbf{X}'_k)/2$, one of their midpoints, which houses the interference pattern. There will be no doubt about the localization of a coherent state, which is captured by a section close to \mathbf{X}'_j , but a section passing near a midpoint will not determine where the interference pattern is coming from. Indeed, the spatial frequency of the oscillations within the section will depend only on the projection $(\mathbf{X}'_j - \mathbf{X}'_k)_1$, leaving $(\mathbf{X}'_j - \mathbf{X}'_k)$ completely undetermined.

There is little change between a classical section near an isolated coherent state and a quantum section, i.e. a huwi function. Indeed, integrating over the product of Gaussians in (1.2) produces a new Gaussian in the \mathbf{x}_1 -plane, centred on \mathbf{X}'_{a1} or \mathbf{X}'_{b1} . However, if \mathbf{X}' lies near $(\mathbf{X}'_a + \mathbf{X}'_b)/2$, the interference term is dampened by a factor $\exp[-(\mathbf{X}'_a - \mathbf{X}'_b)^2/\hbar]$, so that it is not visible unless both section planes, \mathbf{X}'_a and \mathbf{X}'_b , lie close to each other. Of course, this cancellation of interference is a familiar feature of Husimi functions and merely reflects the Husimi side of the hybrid huwi representation. The Wigner side arises if \mathbf{X}'_a and \mathbf{X}'_b are nearly the same. Then, there will be practically no cancellation of the interference pattern in the \mathbf{x}_1 -plane, i.e. the huwi function will resemble the classical section of the Wigner function, with two classical maxima and a central interference pattern.

It might seem too severe a restriction only to observe interferences of structures that lie on two-dimensional sections, but it is important to recall that the Wigner function is symplectically invariant; that is, for any classical linear canonical transformation, $\mathbf{x} \mapsto \mathbf{x}'$, the effect of the corresponding unitary quantum transformation is $W(\mathbf{x}) \mapsto W(\mathbf{x}')$ (e.g. [Voros 1977](#)). Thus, it is always possible to picture the interference pattern between a pair of coherent states by effecting a symplectic transformation that includes them both in the same two-dimensional plane. On the other hand, the overlapping interference pattern for the superposition of a large number of coherent states will be vastly simplified in the huwi representation, without reaching the extreme of the Husimi function itself.

In short, a superposition of coherent states is a simple system useful to illustrate the huwi representation. Fortunately, many of the simple features here can also be identified in the context of the more elaborate geometries treated in the following sections. One can proceed to a more detailed investigation of superposition of arbitrarily squeezed and rotated coherent states, but it all reduces to performing Gaussian integrals and the qualitative result is unchanged. The huwi representation for a Schrödinger cat state is displayed as a Gaussian for any coherent state, which lies on the section plane, $\mathbf{x}' = \mathbf{X}'$; however, the interference pattern persists, if and only if both coherent states lie on this plane ([figure 1](#)).

4. Van Vleck states

Let us now consider wave functions $\langle q|\psi\rangle$, corresponding to the common eigenstates of L commuting observables, \hat{I}_l . These may be described in the semiclassical limit as being supported by an L -dimensional Lagrangian ψ -surface in the $(2L)$ -dimensional phase space ([Arnold 1978](#)), obtained as the intersection of the level surfaces for the functions, $I_l(\mathbf{x})$, corresponding to the

observables. Locally, each branch of this surface is obtained by the action

$$p^j(q) = \frac{\partial S^j(q)}{\partial q}, \tag{4.1}$$

and the full wave function is then a superposition of the various branches,

$$\langle q|\psi\rangle \approx \sum_j a^j(q)\exp\left[\frac{i}{\hbar}S^j(q)\right]. \tag{4.2}$$

In the case of a bound state, i.e. that these common eigenstates form a discrete spectrum, the ψ -surface is an L -dimensional torus (Arnold 1978), characterized by L independent irreducible circuits. All such closed curves on the ψ -surface should satisfy Bohr–Sommerfeld quantization rules, i.e.

$$\oint_{\psi} p \cdot dq = \left(n_l + \frac{1}{2}\right)2\pi\hbar. \tag{4.3}$$

The amplitudes, defined as

$$a^j(q) = \left|\det\frac{\partial^2 S^j}{\partial q\partial I}\right|^{-1/2}, \tag{4.4}$$

except for a global normalization factor, are finite except at caustics (generalized turning points), where the branches of the function $S^j(q)$ are joined.

This generalization of simple Wentzel–Kramers–Brillouin (WKB) states to higher dimensions and their evolution was originally derived by Van Vleck (1928) and various further improvements are reviewed, for instance, in Maslov & Fedoriuk (1981), Ozorio de Almeida (1988) or Gutzwiller (1990). One should note that the geometric definition of each branch of the Lagrangian surface in (4.1) is unaffected by the addition of a j -dependent constant, but this *Maslov correction* will not concern us here. The semiclassical approximation to the wave function breaks down at caustics, but these can be shifted by symplectic transformations, as discussed in §3. The simplest example is the phase space rotation by $\pi/2$, which amounts to exchanging the position for the momentum wave function, known as the *Maslov method* (Maslov & Fedoriuk 1981).

The semiclassical form of the Wigner function for generalized WKB states was derived by Berry (1977a), but, rather than obtaining the huwi function by its integration with a Gaussian window, it is simpler to start from (2.5) and (4.2) to calculate the reduced wave function

$$\begin{aligned} &\langle \mathbf{X}'|\psi\rangle(q_1) \\ &\approx \sum_j \int dq' \frac{a^j(q_1, q')}{(\pi\hbar)^{(L-1)/4}} \exp\left[-\frac{1}{2\hbar}(q' - Q')^2 - \frac{i}{\hbar}P' \cdot \left(q' - \frac{Q'}{2}\right) + \frac{i}{\hbar}S^j(q_1, q')\right]. \end{aligned} \tag{4.5}$$

The Gaussian factor in the integrand allows us to expand the action around Q' approximately as

$$S^j(q_1, q') \approx S^j(q_1, Q') + p^{j'} \cdot (q' - Q') + \frac{1}{2}(q' - Q') \cdot \mathbf{S}^j \cdot (q' - Q'), \tag{4.6}$$

where

$$p^{j'}(q_1, Q') = \frac{\partial S^j}{\partial q'}(q_1, q' = Q') \tag{4.7}$$

and

$$S^j(q_1, Q') = \frac{\partial^2 S^j}{\partial q' \partial q'}(q_1, q' = Q') \tag{4.8}$$

is an $(L-1) \times (L-1)$ matrix.

Then, (4.5) reduces to the Fourier integral of a Gaussian, if the slow variation of $a^j(q_1, q')$ is neglected, i.e.

$$\begin{aligned} \langle \mathbf{X}' | \psi \rangle(q_1) \approx & \sum_j (4\pi\hbar)^{(L-1)/4} a^j(q_1, Q') [\det \mathbf{M}^j]^{1/2} \\ & \times \exp \left[-\frac{1}{2\hbar} (p^{j'} - P') \cdot \mathbf{M}^j \cdot (p^{j'} - P') - \frac{i}{2\hbar} P' \cdot Q' + \frac{i}{\hbar} S^j(q_1, Q') \right], \end{aligned} \tag{4.9}$$

where the $(L-1) \times (L-1)$ matrix,

$$\mathbf{M}^j = [\mathbf{I} - i\mathbf{S}^j]^{-1}, \tag{4.10}$$

and $p^{j'}$ are functions of both q_1 and the parameter Q' .

The generic situation is that a given section plane may intersect the ψ -surface at isolated points, because the \mathbf{X}' -plane is two-dimensional and the ψ -surface is L -dimensional. Thus, for $L=2$, we have generic point intersections, for regions of \mathbf{X}' that have a finite (Lebesgue) measure. For $L>2$, intersections again occur generically at isolated points, but only for the section parameters in the \mathbf{X}' -projection of the ψ -surface.³ The above wave function is localized in the neighbourhood of the positions that correspond to the intersections of the \mathbf{X}' -plane with the ψ -surface, i.e. the points $q_1 = Q_1^j$, defined by the equation $p^{j'}(Q_1^j, Q') = P'$. Consistent local expansions of the action, $S^j(q_1, Q')$, around each of these points then lead to the simplified expression

$$\langle \mathbf{X}' | \psi \rangle(q_1) \approx \sum_j A^j(\mathbf{X}') \exp \left[-\frac{1}{2\hbar} \Omega^j (q_1 - Q_1^j)^2 + \frac{i}{\hbar} p_1^j (q_1 - Q_1^j) \right], \tag{4.11}$$

where

$$p_1^j = \frac{\partial S^j}{\partial q_1}(Q_1^j, Q'), \tag{4.12}$$

$$A^j(\mathbf{X}') = (4\pi\hbar)^{(L-1)/4} a^j(Q_1^j, Q') [\det \mathbf{M}^j]^{1/2} \exp \left[-\frac{i}{2\hbar} P' \cdot Q' + \frac{i}{\hbar} S^j(Q_1^j, Q') \right] \tag{4.13}$$

and

$$\Omega^j(q_1^j, Q') = \left(\frac{\partial p^{j'}}{\partial q_1} \right)^T \cdot \mathbf{M}^j \cdot \frac{\partial p^{j'}}{\partial q_1} + i \frac{\partial^2 S^j}{\partial q_1 \partial q_1}. \tag{4.14}$$

³The situation is quite analogous to the intersections of a given curve with a set of parallel lines in three dimensions.

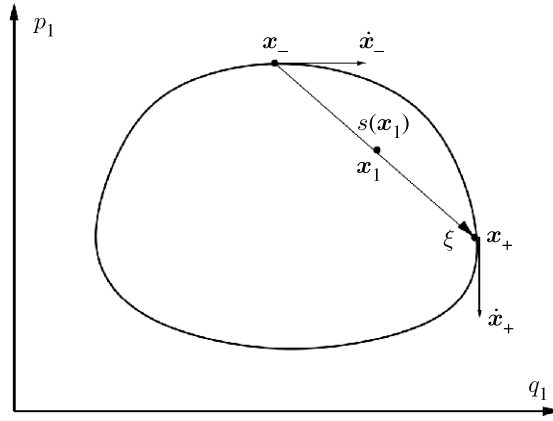


Figure 2. A single chord, ξ , is centred on \mathbf{x}_1 if it is close to a convex quantized curve in the case of one degree of freedom. The phase of the Wigner function is proportional to the area $s(\mathbf{x}_1)$ between the chord and the shell, while the amplitude, $\alpha(\mathbf{x}_1)$, depends on both phase space velocities at the tips of ξ . A caustic results from parallel tangents at the chord tips.

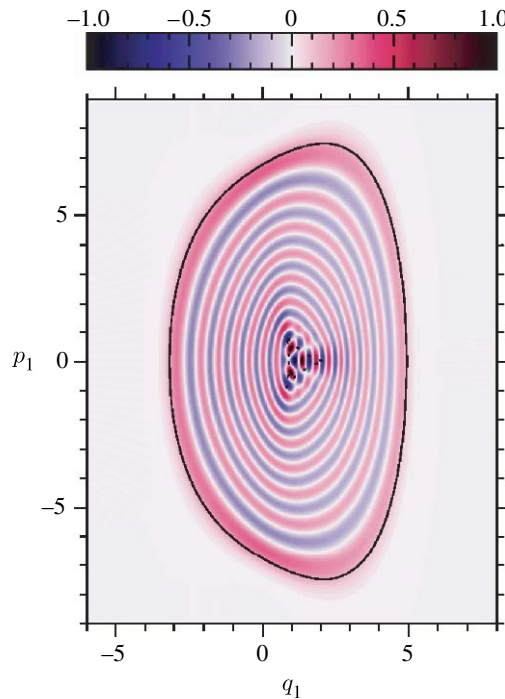


Figure 3. The Wigner function of an $L=1$ degree of freedom. system associated with a quantized ψ_1 -curve (the continuous line). Inside the Wigner caustic (the dotted line), the interference pattern comes from the presence of three chords for each phase space point $\mathbf{x}_1 \equiv (p_1, q_1)$.

Thus, the reduced wave function obtained from a Van Vleck state by a quantum section is approximately a superposition of generalized coherent states, albeit each is squeezed and rotated in the way specified by the complex number \mathcal{Q}^j .

The huwi representation can then generically be approximated by a Schrödinger cat state, with the generalized coherent states placed on the \mathbf{x}_1 -projection of the points of intersection of the ψ -surface with the section plane. This is similar to the states considered in §3. The main difference is that, for $L=2$, variations of the \mathbf{X}' -section plane lead to similar patterns in the case of Van Vleck states, because these also intersect the ψ -surface. By contrast, the huwi representation of cat states changes drastically depending on whether the section plane comes close to any of the localized states within the full phase space. Also, it will be unusual for a higher dimensional cat to have more than one coherent state sampled by a given \mathbf{X}' -section, whereas the general huwi representation of a Van Vleck state, for $L=2$, is a full cat with its interference patterns at all the midpoints.

Let us contrast this to the semiclassical Wigner function for $L=1$ (Berry 1977a),

$$W_1(\mathbf{x}_1) \approx \sum_k \alpha^k(\mathbf{x}_1) \cos \frac{s^k(\mathbf{x}_1)}{\hbar}, \quad (4.15)$$

corresponding to the generalized WKB state (4.2). The sum in (4.15) runs over all chords on the ψ_1 -curve that are centred on \mathbf{x}_1 and s^k is the area between the chord and the shell (plus a semiclassically small Maslov phase), as shown in figure 2. The semiclassical approximation (4.15) breaks down along caustics, where the amplitudes α^k display spurious divergences. The caustics of Wigner functions are the loci of coalescing chords. It is remarkable that the above approximation for the Wigner function of a bound state is only self-consistent if the ψ -curve is quantized according to the Bohr–Sommerfeld rule (4.3), as shown by Berry (1977a), the same condition that needs to be imposed on (4.2).

Figure 3 displays an example of the Wigner function for an eigenstate of the Hamiltonian, $H(\mathbf{x}_1) = p_1^2/2 + (q_1 - 4)^2/2 + 0.05q_1^4$, computed numerically. The semiclassical structure described above is clearly discernible. The quantized ψ_1 -curve is a uniform maximum with a constant phase, and within it there lie a succession of constant phase rings. In this region, there is only one chord, $\xi(\mathbf{x})$. It is remarkable that the relation of the interference pattern, at any point \mathbf{x} in the interior of the curve, to the chord, $\xi(\mathbf{x})$, is quite analogous to that between the interference fringes of a Schrödinger cat and the vector that separates the pair of coherent states; the analogy holds for the direction of the fringes and their spatial frequency. Indeed, it is possible to fit the semiclassical state quite accurately by a generalized cat state with a discrete set of coherent states along the quantized curve (Kenfack et al. 2004; Carvalho et al. in preparation). Evidently, the phase difference between the pair of coherent states at the chord tips must then agree with $s(\mathbf{x}_1)$, the area between the chord and the quantized curve.

The states described by such Wigner functions also arise in higher dimensions from the intersection of the \mathbf{X}' -plane and the ψ -surface with a product torus, corresponding to a product state, $|\psi\rangle = |\psi_1\rangle \otimes |\psi'\rangle$ (Ozorio de Almeida & Hannay 1982). This intersection is ungeneric because it specifies a continuous curve rather than isolated points. Even tori that are not products will produce huwi functions in the standard form of (4.15) if this is generated by the overlap with a position state $|Q'\rangle$, considered as the limit of the squeezed state. Evidently, fixing $q' = Q'$ in (4.2) generates the semiclassical wave function

$$\langle Q'|\psi\rangle(q_1) = \langle q_1, Q'|\psi\rangle \approx \sum_j a^j(q_1, Q') \exp \left[\frac{i}{\hbar} S^j(q_1, Q') \right], \quad (4.16)$$

which is also of the WKB form. Moreover, because the torus is a Lagrangian surface, all the different $(2L-1)$ -dimensional sections, defined by each Q' , must intersect the torus along quantized closed curves, i.e. satisfying (4.3). Therefore, each of the corresponding Wigner functions, $hw_{Q'}(\mathbf{x}_1)$, has the usual form of (4.15).

In §5, we display computational evidence that the huwi function of chaotic quantum states resembles, in some aspects, semiclassical Wigner functions of bound states of systems with a single degree of freedom.

5. Numerical study of eigenstates of a chaotic system

In a fully classical chaotic system, the simplest invariant structures in the phase space are the periodic orbits and the full energy shell, with a typical trajectory sweeping all this $(2l-1)$ -dimensional surface (i.e. ergodic motion). Indeed, more complex fractal invariant subsets may be described in terms of their unstable periodic orbits, together with the homoclinic and heteroclinic orbits on the intersections of their stable and unstable manifolds. These invariant structures should be the skeleton for the construction of a semiclassical theory for the quantum energy eigenstates, which has been sought over the last 40 years. The intersection of the two-dimensional \mathbf{X}' -plane with a compact $(2L-1)$ -dimensional energy shell of a bound classical system produces a closed curve in the \mathbf{x}_1 -plane, for all $L > 1$. Therefore, it is the interference of this classical structure within the section that should determine the huwi representation for each parameter \mathbf{X}' .

Viewed as a pure state for $L=1$, this is a type of Wigner function that has not been previously studied. A resemblance to the simple semiclassical Wigner function presented at the end of §4 may be anticipated; the chords, $\xi(\mathbf{x})$, on the section curve should lead to interference fringes parallel to the chord, just as in the WKB case. The main freedom for variations lies in the way this phase is shifted, as the centre \mathbf{x} is displaced.⁴

Nonetheless, our semiclassical intuition cannot be pushed too far. The huwi function results from a *thick* quantum section, rather than a *thin* classical section, so that a neighbourhood of the full Wigner function is involved. Furthermore, we must deal with a continuum of \mathbf{X}' -parametrized Wigner functions. The corresponding classical sections cannot all be Bohr-quantized, so that the self-consistency of the simple semiclassical theory for these states must be broken.

In the absence of a full semiclassical theory for chaotic eigenstates, we resort to numerical calculations of the huwi function for a particular system. The classical *Nelson Hamiltonian* is defined as (Baranger & Davies 1987)

$$H(\mathbf{x}_1, \mathbf{x}_2) = \frac{p_1^2 + p_2^2}{2} + \frac{\omega_1^2 q_1^2}{2} + \omega_2 \left(q_2 - \frac{q_1^2}{2} \right)^2, \quad (5.1)$$

where $\omega_1^2 = 0.1$ and $\omega_2 = 1$, and its quantum counterpart results from the replacement $\mathbf{x}_1 \equiv (q_1, p_1) \rightarrow (\hat{q}_1, \hat{p}_1)$ and $\mathbf{x}_2 \equiv (q_2, p_2) \rightarrow (\hat{q}_2, \hat{p}_2)$ in (5.1). The restriction of the classical Hamiltonian (5.1) to the two-dimensional \mathbf{X}' -planes $q_1 = Q'$ and $p_1 = P'$ defines harmonic oscillators in the \mathbf{x}_2 variables, $h_2(\mathbf{x}_2) = H(\mathbf{X}', \mathbf{x}_2)$. The classical trajectories of this harmonic oscillator coincide with the

⁴The amplitude that can be attributed to the tips of each chord lying on the classical section may also vary. In the extreme case where this is concentrated in the neighbourhood of a discrete set of points, the huwi function should again resemble the Wigner function of a Schrödinger cat state.

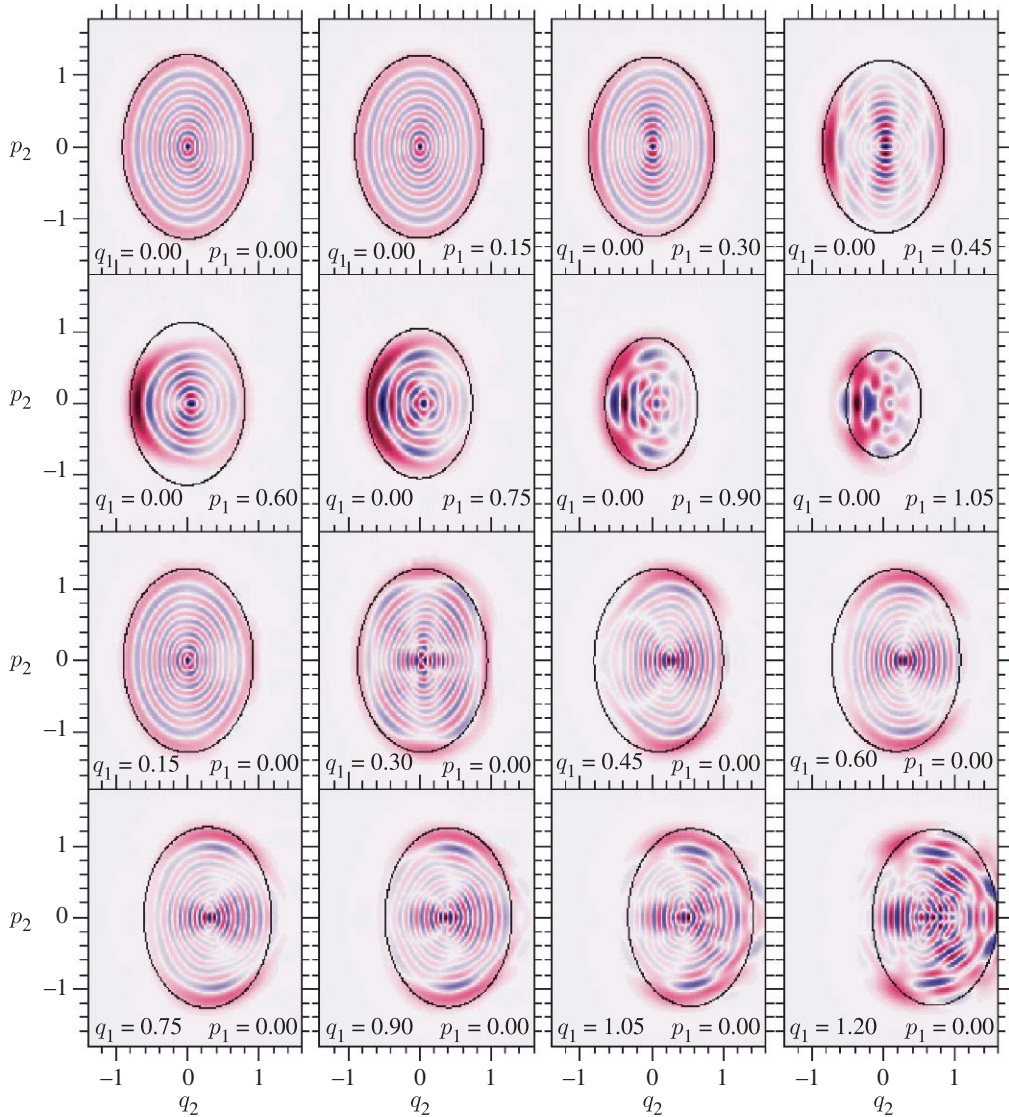


Figure 4. The huwi functions for the eigenstate $|\psi_{n=311}\rangle$ of the Nelson Hamiltonian in different two-dimensional planes $q_1 = Q'$ and $p_1 = P'$. The black closed curve in each graph is the intersection of the energy shell with the specified two-dimensional plane for the eigenenergy $E_{311} \approx 0.836$. This is the classical trajectory of the harmonic oscillator Hamiltonian obtained by restricting the original Hamiltonian to that plane. We do not use a common scale for the intensities in all the graphs in order to clearly display the structure of the huwi functions in each plane.

intersection of the energy shell of the full Hamiltonian with the planes $q_1 = Q'$ and $p_1 = P'$. The alternative classical sections $\mathbf{x}_2 = \mathbf{X}'$ on (5.1) defines anharmonic oscillators, $h_1(\mathbf{x}_1) = H(\mathbf{x}_1, \mathbf{X}')$, whose closed trajectories are not ellipses.

The classical dynamics of this system has been studied in considerable depth. Instead of merely relying on the Poincaré section for a few typical trajectories (exhibited in Ribeiro *et al.* (2004)), Baranger & Davies (1987; see also Prado & de Aguiar 1994 and references therein) made extensive studies of a large number

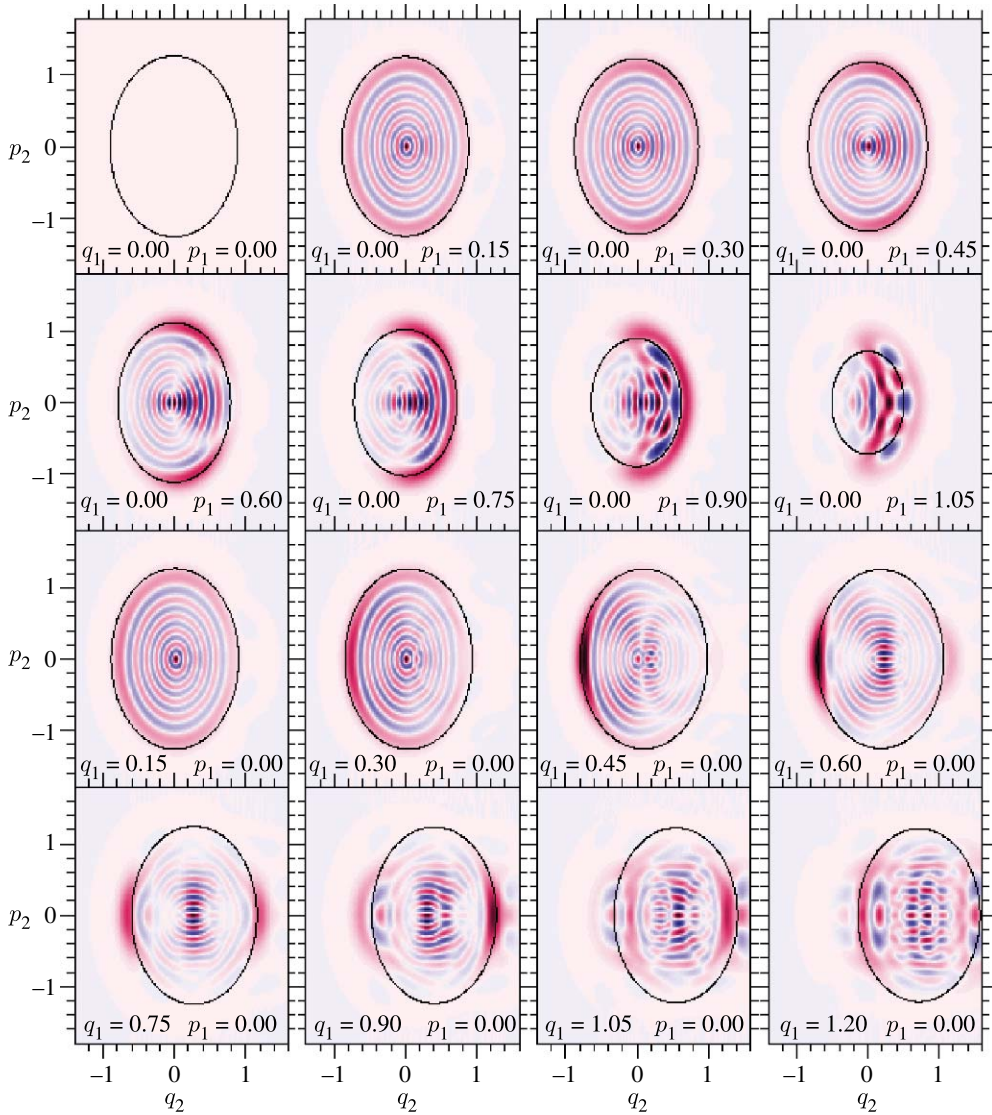


Figure 5. The huwi functions for the energy eigenstate $|\psi_{n=294}\rangle$ ($E_{294} \approx 0.813$) of the Nelson Hamiltonian. Note that the huwi function is null, in the symmetry plane $\mathbf{x}_1 = \mathbf{X}' = (0, 0)$, because its definition involves the partial projection $\langle \mathbf{X}' | \psi_{294} \rangle$ of an even coherent state $|\mathbf{X}'\rangle$ with an odd $|\psi_{294}\rangle$ state in the \mathbf{x}_1 degree of freedom. We do not use a common scale for the intensities in all the graphs in order to clearly display the structure of the huwi functions in each plane.

of the periodic orbits with a relatively low period and their elaborate bifurcation trees as a function of energy. It was possible to follow these families of periodic orbits as they became unstable in an energy range above $E=0.3$, though a few recovered stability at $E \approx 10$. All quantum states depicted here were calculated in an energy window of $0.81 < E < 0.84$, where it can be guaranteed that only orbits of very high periods may be stable. Hence, the knowledge of the general pattern for the dynamics from the skeleton of periodic orbits precludes any stability

islands that are not very thin, so that the system is nearly ergodic. The choice of $\hbar = 0.05$ allows us to compute the eigenstates in the energy range corresponding to (quasi-)chaotic motion for this classical Hamiltonian. It will be observed in figures 4–6 that this choice for the relative value of Planck’s constant is sufficiently small for us to distinguish the qualitative features of the quantum sections from those of quantized curves. However, these computations do not reach an asymptotic semiclassical regime.

It would be natural to use a harmonic oscillator basis for calculating those of the Nelson Hamiltonian, but it is more efficient to use a basis of *distorted oscillators* (Toscano et al. 2001). In figures 4–6, we show the huwi function of three different eigenstates for several constant \mathbf{x}_1 -planes. It should be observed that, in spite of varying degrees of irregularity in the internal fringe pattern among these examples, the wavelength is larger for the smaller classical curves, which hence have shorter chords. In all cases, the pattern decays outside the classical curve.

It is interesting to compare the huwi functions with thin sections of the full Wigner function of the eigenstates, along the planes $q_1 = Q'$ and $p_1 = P'$, as shown in figure 7, which also compares them to the Husimi functions for the corresponding quantum sections. These sections of the full Wigner function display interference of contributions from different parts of the energy shell outside of the plane section. Semiclassically, these oscillations can be ascribed to chords, $\xi(\mathbf{x})$, with centres, \mathbf{x} , in the section, but with tips on the energy shell far from this plane. This is particularly evident in the region $q_2 > 0$ outside the classical curve. The Gaussian smoothing of (1.2), which defines the huwi function in the planes $q_1 = Q'$ and $p_1 = P'$, washed out all these interference contributions, isolating the contributions from chords with tips lying on the classical curve or in its neighbourhood. Thus, the result is a huwi function with an interference pattern inside the classical curve and exponentially small values outside, which resembles the Wigner functions associated with a quantized curve (figure 2). However, it is clear that the constant phase curves of the interference fringes do not follow exactly the regular concentric pattern of a Wigner function for a quantized curve.

The plane $q_1 = p_1 = 0$ is special for the Nelson Hamiltonian. On the one hand, it is the symmetry plane for the reflection symmetry $q_1 \rightarrow -q_1$ of the system. Thus, the huwi function in this plane discriminates the odd from the even states in the \mathbf{x}_1 degrees of freedom. For the odd states, the huwi function is zero on the plane, because, according to (2.6), it comes from a partial projection on an even coherent state $|\mathbf{X}' = (0, 0)\rangle$. On the other hand, this is a classically invariant plane that contains the *vertical family* of periodic orbits of the full Hamiltonian. In agreement with our choice of energy range such that the motion is basically chaotic, the vertical family of periodic orbits is unstable in this range. Therefore, they give rise to scars as described by Heller (1984), Bogomolny (1988) and Berry (1989), i.e. a collective enhancement of amplitude in a narrow energy range. All the chords with tips on one periodic orbit define the so-called *central surface*, which, in this case, is merely the region in the invariant plane inside the classical vertical orbit (Toscano et al. 2001). When the classical orbit is Bohr (or ‘anti-Bohr’) quantized, it was shown in Toscano et al. (2001) that the mixture of eigenstates in a narrow energy window, i.e. the spectral Wigner function, presents a scar in the central surface of the periodic orbit, which takes the form of a pattern of concentric rings of constant phase, just like those of the semiclassical $L=1$

Wigner function of (4.15). This pattern is also evident for an individual eigenstate, as is the case for $|\psi_{n=305}\rangle$, whose eigenenergy is very close to the Bohr energy (figure 7). In this case, the huwi function in the invariant plane, as a thick section of the Wigner function, simply isolates the scar contribution of the periodic orbit (figure 6). The thickness of the scar is sampled by the huwi functions up to a linear distance of the order $\sqrt{\hbar} \approx 0.22$ by sections parallel to the symmetry plane.

Even when the periodic orbit is far from being Bohr-quantized, the huwi functions around the invariant plane isolates similar contributions from the periodic orbit, as shown in figures 4 and 5. The similarity of these huwi functions with the Wigner functions for harmonic oscillator eigenstates is remarkable, especially if it is recalled that their energies are not Bohr-quantized.

The quantum sections, which are represented by the huwi function, should not be confused with the *quantum Poincaré surface of section* (Leboeuf & Saraceno 1990*a,b*). The latter is a *projection* onto a two-dimensional plane of the Husimi function evaluated along the three-dimensional energy shell. It is an invaluable tool for the study of the classical features of the quantum state. For instance, scarred states (Heller 1984; Bogomolny 1988; Berry 1989) exhibit maxima in the neighbourhood of the points where a periodic orbit crosses the corresponding classical section (e.g. Arranz *et al.* 2004). By contrast, the two-dimensional quantum section corresponds to a classical section that intersects the energy shell along a closed curve. The Husimi representation of this quantum section coincides with the section of the Husimi function of (2.7) and, hence, it is entirely concentrated along the classical curve. Thus, the structure within the classical curve of the huwi function is built up of quantum interferences that are washed out in the Husimi representation of the section, as shown in figure 7.

6. Discussion

The huwi representation displays the classical structure underlying a quantum state that is cut by a given two-dimensional plane, together with the interference pattern due to this two-dimensional structure. The interference effects due to all other classical regions, not sampled by this plane, are deleted. By considering first some simple examples, we have shown that the ensemble of the Wigner functions for such sections constitutes a promising tool for the study of the eigenstates of chaotic systems, whether these be ergodic or scarred to some extent. Moreover, in the case that the full state describes a pair of entangled components, the quantum section describes the state of a subsystem after a well-defined experiment is conceivably realized on the complementary subsystem. The Wigner functions for these resulting states have not been previously studied, to our knowledge.

The Nelson Hamiltonian, whose eigenstates were presented in §5, corresponds to a mixed classical system. At low energies, the motion is a perturbation of the two-dimensional harmonic oscillator, but becomes increasingly chaotic at higher energies. Even though the limit of truly ergodic motion is unlikely ever to be reached, it is expected that most orbits will eventually sweep over most of the energy shell, within the wavelength of the quantum motion for the states that we have considered. Therefore, we expect that most eigenstates will resemble ergodic quantum states.

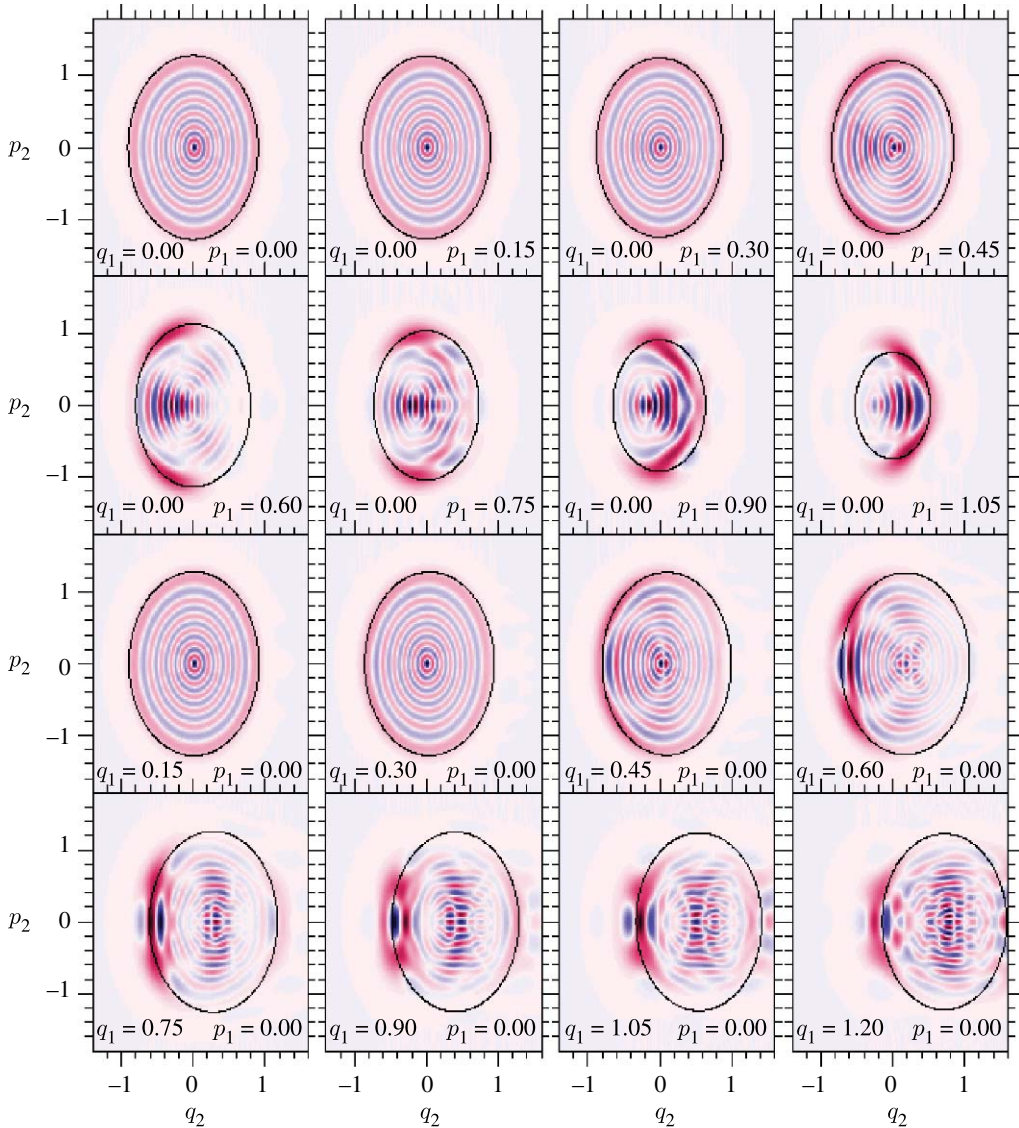


Figure 6. The huwi functions for the eigenstate $|\psi_{n=305}\rangle$. We do not use a common scale for the intensities in all the graphs in order to clearly display the structure of the huwi functions in each plane. Thus, it is not possible to appreciate the enhanced amplitude of the huwi functions around the classically invariant plane $q_1 = p_1 = 0$, which reflects the fact that the Wigner function of this state has a scar of the periodic orbit in this plane (figure 7). The distance of the eigenenergy $E_{305} \approx 0.828$ from the Bohr energy level for the periodic orbit is of the order of a single level spacing, i.e. $\mathcal{O}(\hbar^2)$.

Our computations clearly show that even a partial smoothing of the Wigner function is not concentrated in the neighbourhood of the energy shell. Indeed, each quantum section of the energy shell, sampled by each huwi function, marks the boundary, beyond which the huwi function is vanishingly small. But inside each section of the shell, a closed curve, the huwi function oscillates somewhat like a typical Wigner function of a Bohr-quantized state in the case of a single degree of

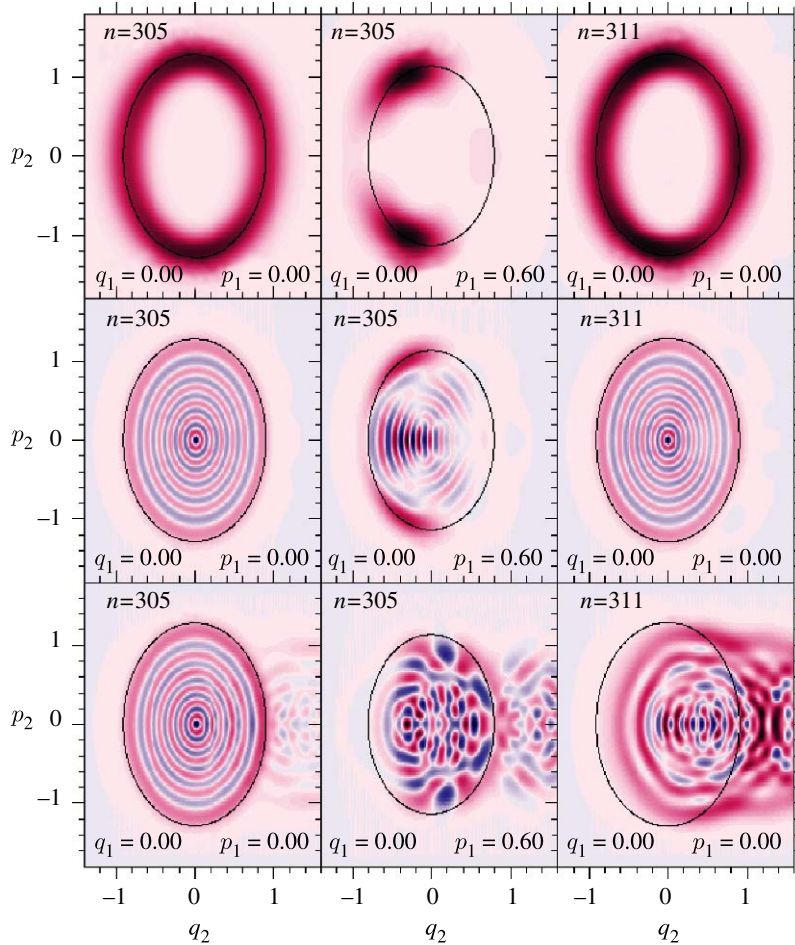


Figure 7. The top row displays the plane sections of the Husimi function for three eigenstates $|\psi_n\rangle$ of the Hamiltonian of (5.1). The energy shell in each plane $q_1 = Q'$ and $p_1 = P'$ is drawn in black (i.e. the classical curve). A comprehensible quantum interference pattern, associated with the classical curve and its surroundings, starts to show up in the corresponding huwi functions displayed in the middle row. However, the corresponding plane sections of the Wigner function in the bottom row have interference contributions of different parts of the energy shell far from these plane sections (particularly evident in the region $q_2 > 0$ outside the classical curve).

freedom. Usually, these are considered as simple examples of eigenstates of integrable systems, though it should not be forgotten that they are also trivially ergodic, a trajectory visits uniformly the entire (one-dimensional) energy shell. Therefore, the huwi representation has brought to light a natural, but unsuspected, family resemblance between ergodic states of all dimensions.

The first difference between quantum sections for chaotic eigenstates and simple Bohr-quantized states is clearly exhibited, not only by the huwi function but also by the Husimi function of the section, i.e. the section of the full Husimi function. In both the cases, this is only appreciable in the neighbourhood of the classical curve, but the intensity of the chaotic Husimi function can exhibit

marked modulations along the curve that vary from section to section, in marked contrast to the regular quantized state.

The second difference, displayed only by the huwi function, concerns the regularity of the wave pattern inside the classical curve. With the exception of huwi functions obtained from very symmetric sections of the energy shell, it was found in §5 that the regular pattern of concentric wavefronts for the Bohr-quantized state in figure 2 may be broken up in many places, even though the direction of the phase curves and their spacing is approximately maintained.

This scenario is curiously reminiscent of a snap shot of dislocations in wave trains, analysed by Nye & Berry (1974). For travelling wave trains, the approximately constant wavelength is a consequence of the approximately constant temporal frequency of an initial pulse. However, the returning signal results from several scattered components with different phases. The outcome is an imperfect wave pulse with dislocations, where constant phase curves are interrupted, just as for an imperfect crystal lattice. Similar structures arise for travelling waves through the spatial and temporal disorder (La Porta & Surko 1996). In the present case, it is the single geometric chord, centred on a given interior point of the classical curve, that specifies the dominant spatial frequency near the centre, as well as the direction of the wavefronts, which must be parallel to the chord. So far, this is the same as holds for the Bohr-quantized curve, but the neighbouring oscillations of the chaotic huwi functions are closer to scattered wave trains than to regular concentric waves. This same general picture can be conjectured for two-dimensional quantum sections of even higher dimensional chaotic energy shells.

Perhaps this is only a very qualitative analogy, though it indicates a direction to be pursued for the systematic characterization of huwi functions obtained from chaotic eigenstates. It is emphasized in Nye & Berry (1974) that the finite size of the pulse is a precondition for the presence of dislocations. In this respect, it should be recalled that diverse types of quantum states can be successfully fitted by localized coherent states placed along the relevant classical manifold, such that the oscillations midway between each pair of phase space Gaussians have the same spatial frequency as that of the fitted state (Kenfack *et al.* 2004; Carvalho *et al.* in preparation). One can then conjecture that the dislocations on the crests of the huwi pattern may be ascribed to the superposition of neighbouring coherent states on the classical curve with arbitrary phases.

We thank Dr Oliver Brodier for an illuminating discussion and one of the referees for his thoughtful criticisms. Partial financial support from the Millenium Institute of Quantum Information, PROSUL, FAPERJ CNPq and UNESCO/IBSP Project 3-BR-06 is gratefully acknowledged. A.K. acknowledges the financial support by the Max-Planck Gesellschaft through the Reimar Lüst fund (Reimar Lüst Fellow 2005) and by the Alexander von Humboldt foundation with research grant no. IV. 4-KAM 1068533 STP.

References

- Arnold, V. I. 1978 *Mathematical methods of classical mechanics*. Berlin, Germany: Springer.
- Arranz, F. J., Benito, R. M. & Borondo, F. 2004 Topology of the distribution of zeros of the Husimi function in the LiNC/LiCN molecular system. *J. Chem. Phys.* **120**, 6516–6523. (doi:10.1063/1.1665984)

- Arthurs, E. & Kelly Jr, J. L. 1965 On the simultaneous measurement of a pair of conjugate observables. *Bell Syst. Tech. J.* **44**, 725.
- Baranger, M. & Davies, K. T. R. 1987 Periodic trajectories for a two-dimensional nonintegrable Hamiltonian. *Ann. Phys. (NY)* **177**, 330. (doi:10.1016/0003-4916(87)90123-0)
- Berry, M. V. 1977a Semi-classical mechanics in phase space: a study of wigner's function. *Phil. Trans. R. Soc. A* **287**, 237–271. (doi:10.1098/rsta.1977.0145)
- Berry, M. V. 1977b Regular and irregular semiclassical wavefunctions. *J. Phys. A* **10**, 2083–2092. (doi:10.1088/0305-4470/10/12/016)
- Berry, M. V. 1989 Quantum scars of classical closed orbits in phase space. *Proc. R. Soc. A* **423**, 219–231. (doi:10.1098/rspa.1989.0052)
- Bogomolny, E. B. 1988 Smoothed wave functions of chaotic quantum systems. *Physica D* **31**, 169–189. (doi:10.1016/0167-2789(88)90075-9)
- Carvalho, A. R. R., Kenfack, A., Ozorio de Almeida, A. M., Rost, J. M. & Toscano, F. In preparation. Representation of chaotic eigenstates by Gaussians in phase space.
- Cohen Tannoudji, C., Diu, B. & Laloë, F. 1977 *Quantum mechanics*. New York, NY: Wiley.
- Colin de Verdière, Y. 1985 Ergodicité et fonctions propres du laplacien. *Comm. Math. Phys.* **102**, 497–502. (doi:10.1007/BF01209296)
- Glauber, R. J. 1963 Photon correlations. *Phys. Rev. Lett.* **10**, 84–86. (doi:10.1103/PhysRevLett.10.84)
- Goldstein, H. 1980 *Classical mechanics*, 2nd edn. Reading, MA: Addison-Wesley.
- Gutzwiller, M. 1990 *Chaos in classical and quantum mechanics*. New York, NY: Springer.
- Hannay, J. H. 1998 The chaotic analytic function. *J. Phys. A* **31**, L755–L762. (doi:10.1088/0305-4470/31/49/001)
- Heller, E. J. 1984 Bound-state eigenfunctions of classically chaotic hamiltonian systems: scars of periodic orbits. *Phys. Rev. Lett.* **53**, 1515–1518. (doi:10.1103/PhysRevLett.53.1515)
- Howell, J. C., Bennink, R. S., Bentley, S. J. & Boyd, R. W. 2004 Realization of the Einstein–Podolsky–Rosen paradox using momentum and position entangled photons from spontaneous parametric down conversion. *Phys. Rev. Lett.* **92**, 210 403. (doi:10.1103/PhysRevLett.92.210403)
- Husimi, K. 1940 Some formal properties of the density matrix. *Proc. Phys. Math. Soc. Jpn* **22**, 264.
- Kenfack, A., Rost, J. M. & Ozorio de Almeida, A. M. 2004 Optimal representations of quantum states by Gaussians in phase space. *J. Phys. B* **37**, 1645. (doi:10.1088/0953-4075/37/8/007)
- Klauder, J. R. & Skagerstam, B.-S. 1985 *Coherent states, applications to physics and mathematical physics*. Singapore: World Scientific.
- Kurchan, J., Leboeuf, P. & Saraceno, M. 1989 Semiclassical approximations in the coherent state representation. *Phys. Rev. A* **40**, 6800. (doi:10.1103/PhysRevA.40.6800)
- La Porta, A. & Surko, C. M. 1996 Phase defects as a measure of disorder in traveling-wave convection. *Phys. Rev. Lett.* **77**, 2678–2681. (doi:10.1103/PhysRevLett.77.2678)
- Leboeuf, P. & Saraceno, M. 1990a Eigenfunctions of non-integrable systems in generalised phase spaces. *J. Phys. A* **23**, 1745–1764. (doi:10.1088/0305-4470/23/10/016)
- Leboeuf, P. & Saraceno, M. 1990b Structure of eigenfunctions in terms of classical trajectories in an SU(3) schematic shell model. *Phys. Rev. A* **41**, 4614–4624. (doi:10.1103/PhysRevA.41.4614)
- Leboeuf, P. & Voros, A. 1990 Chaos-revealing multiplicative representation of quantum eigenstates. *J. Phys. A* **23**, 1765–1774. (doi:10.1088/0305-4470/23/10/017)
- Leboeuf, P. & Voros, A. 1995 In *Quantum chaos: between order and disorder* (eds G. Casati & B. Chirikov), p. 507. Cambridge, UK: Cambridge University Press.
- Leonhardt, U. 1997 *Measuring the quantum state of light*, p. 507. Cambridge, UK: Cambridge University Press.
- Maslov, V. P. & Fedoriuk, M. V. 1981 *Semiclassical approximation in quantum mechanics* (transl. from original Russian edition, 1965). Dordrecht, The Netherlands: Reidel.
- Mintert, F., Carvalho, A. R. R., Marek, K. & Buchleitner, A. 2005 Measures and dynamics of entangled states. *Phys. Rep.* **15**, 207. (doi:10.1016/j.physrep.2005.04.006)
- Nye, J. F. & Berry, M. V. 1974 Dislocations in wave trains. *Proc. R. Soc. A* **336**, 165–190. (doi:10.1098/rspa.1974.0012)

- Ozorio de Almeida, A. M. 1988 *Hamiltonian systems: chaos and quantization*. Cambridge, UK: Cambridge University Press.
- Ozorio de Almeida, A. M. 1998 The Weyl representation in classical and quantum mechanics. *Phys. Rep.* **295**, 265–342. (doi:10.1016/S0370-1573(97)00070-7)
- Ozorio de Almeida, A. M. 2006 Entanglement in phase space. In *Theoretical foundations of quantum information* (eds A. Buchleitner & C. Viviescas). Lecture Notes in Physics, Berlin, Germany: Springer. (<http://arxiv.org/abs/quant-ph/0612029>)
- Ozorio de Almeida, A. M. & Hannay, J. 1982 Geometry of two dimensional tori in phase space: projections, sections and the Wigner function. *Ann. Phys.* **138**, 115–154. (doi:10.1016/0003-4916(82)90177-4)
- Ozorio de Almeida, A. M., Vallejos, R. O. & Saraceno, M. 2004 Pure state correlations: chords in phase space. *J. Phys. A* **38**, 1473–1490. (doi:10.1088/0305-4470/38/7/005)
- Perelomov, A. 1986 *Generalized coherent states and their applications*. New York, NY: Springer.
- Prado, S. P. & de Aguiar, M. A. M. 1994 Effects of symmetry breakdown in the bifurcations of periodic orbits of a nonintegrable Hamiltonian system. *Ann. Phys. (NY)* **231**, 290–310. (doi:10.1006/aphy.1994.1044)
- Ribeiro, A. D., de Aguiar, M. A. M. & Baranger, M. 2004 Semiclassical approximations based on complex trajectories. *Phys. Rev. E* **69**, 66 204. (doi:10.1103/PhysRevE.69.066204)
- Royer, A. 1977 Wigner function as the expectation value of a parity operator. *Phys. Rev. A* **15**, 449–450. (doi:10.1103/PhysRevA.15.449)
- Schanz, H. 2005 Phase-space correlations of chaotic eigenstates. *Phys. Rev. Lett.* **94**, 134 101. (doi:10.1103/PhysRevLett.94.134101)
- Schleich, P. W. 2001 *Quantum optics in phase space*. Berlin, Germany: Wiley-VCH.
- Shnirelman, A. 1974 Ergodic properties of eigenfunctions. *Uspekhi Mat. Nauk.* **29**, 181–182.
- Sudarshan, E. C. G. 1963 Equivalence of semiclassical and quantum mechanical descriptions of statistical light beams. *Phys. Rev. Lett.* **10**, 277–279. (doi:10.1103/PhysRevLett.10.277)
- Takahashi, K. 1986 Wigner and Husimi functions in quantum mechanics. *J. Phys. Soc. Jpn* **55**, 762–779. (doi:10.1143/JPSJ.55.762)
- Toscano, F. & Ozorio de Almeida, A. M. 1999 Geometrical approach to the distribution of the zeros for the Husimi function. *J. Phys. A* **32**, 6321–6346. (doi:10.1088/0305-4470/32/35/310)
- Toscano, F., de Aguiar, M. A. M. & Ozorio de Almeida, A. M. 2001 Scars of the Wigner function. *Phys. Rev. Lett.* **86**, 59–62. (doi:10.1103/PhysRevLett.86.59)
- Van Vleck, J. H. 1928 The correspondence principle in the statistical interpretation of quantum mechanics. *Proc. Natl Acad. Sci. USA* **14**, 178. (doi:10.1073/pnas.14.2.178)
- Voros, A. 1976 Semi-classical approximations. *Ann. Inst. Henri Poincaré* **24A**, 31.
- Voros, A. 1977 Asymptotic h-expansions of stationary quantum states. *Ann. Inst. Henri Poincaré* **24A**, 343.
- Wigner, E. P. 1932 On the quantum correction for thermodynamic equilibrium. *Phys. Rev.* **40**, 749–759. (doi:10.1103/PhysRev.40.749)
- Zelditch, S. 1987 Uniform distribution of eigenfunctions on compact hyperbolic surfaces. *Duke Math. J.* **55**, 919–941. (doi:10.1215/S0012-7094-87-05546-3)
- Zurek, W. H. 2001 Sub-planck structure in phase space and its relevance for quantum decoherence. *Nature* **412**, 712–717. (doi:10.1038/35089017)